Chromatic polynomials of large triangular lattices

1987 J. Phys. A: Math. Gen. 20 5241

(http://iopscience.iop.org/0305-4470/20/15/037)

J. Phys. A: Math. Gen. **20** (1987) 5241-5261. Printed in the UK

Chromatic polynomials of large triangular lattices

R J Baxter

Research School of Physical Sciences, The Australian National University, Canberra, ACT 2601, Australia

Received 24 December 1986

Abstract. Evaluating the q colourings of a lattice is equivalent to solving the q-state zero-temperature antiferromagnetic Potts model. This has recently been done exactly for an infinite triangular lattice with q real. Here the results are extended to the full complex q plane, giving the limiting distribution of the zeros of the chromatic polynomial. The results are compared with finite lattice calculations and the occurrence of isolated real zeros converging on the Beraha numbers is noted.

1. Introduction

Let $Z_N(q; G)$, or simply $Z_N(q)$, be the number of ways of colouring the sites of a graph G of N sites with q colours, no two adjacent sites having the same colour. For instance, if G is a triangle (three sites with each pair connected), then $Z_N(q) = q(q-1)(q-2)$. In general, $Z(q)$ is a polynomial in q of degree N. It is known as the 'chromatic' polynomial.

Chromatic polynomials have been of interest in graph theory for many years (Tutte 1982, Biggs 1976). They are also of interest in physics, where we can regard the colours as states. Then $Z_N(q)$ is the partition function of a model where each site can be in one of q states; adjacent sites must be in different states. This is the zero-temperature limit of the antiferromagnetic Potts model (Wu 1982, Baxter 1982). In this context one usually focuses on the case when G is a large regular lattice.

From both points of view it is interesting to study the zeros of $Z_N(q)$ in the complex q plane. There is a fascinating graph-theoretical conjecture (Beraha *et al* 1978, 1979, 1980) that some of the real zeros of $Z_N(q)$ occur (in the limit of G large) at the 'Beraha numbers'

$$q = 2 + 2\cos(2\pi/r) \qquad r = 2, 3, 4, \ldots \tag{1.1}$$

The first three of these are $q = 0, 1, 2$, which are certainly very special cases of the Potts model ($q = 2$ is the Ising case). The next is the golden number $q = (3+\sqrt{5})/2 \simeq 2.618$, which case has been studied by Tutte (1970, 1973). The Potts model can be related to a staggered six-vertex model (Baxter *et al* 1976) by a transformation that introduces a parameter θ defined by

$$q = 2 + 2\cos\theta \qquad 0 \leqslant \mathrm{Re}(\theta) \leqslant \pi \tag{1.2}$$

so we see that the Beraha numbers correspond simply to $\theta = 2\pi/n$.

There is a considerable literature in physics on zeros of the partition function (Lee and Yang 1952, Asano 1970, Ruelle 1971, 1973, Suzuki and Fisher 1971, Thompson

0305-4470/87/155241+21$02.50

1972, Monroe 1982, 1983, Glasser *et al* 1987a, b). They are a powerful way of studying the analyticity properties of the free energy and locating critical points.

In a previous paper (Baxter 1986), an equivalence of Nienhuis (1982, 1984) was used to relate the chromatic polynomial of the triangular lattice of N sites to the partition function of a loop model on the honeycomb lattice of $2N$ sites. This latter problem is a special case of the Izergin and Korepin (1981) model. It can be solved by the Bethe ansatz method, which gives the 'partition function per site'

$$W(q) = \lim_{N\to\infty} Z_N(q)^{1/N} \tag{1.3}$$

the limit being taken through lattices large in both directions.

More precisely, as is explained in § 3, the method gives the nth root of one of the eigenvalues Λ_1 of the transfer matrix (n being the number of columns of the lattice). Provided Λ_1 is the largest eigenvalue (in modulus), the result is $W(q)$.

For q large it is easy to verify that Λ_1 is the largest eigenvalue. For q finite and complex the author knows of no tractable rigorous method of establishing if it is so. In order to answer this question, we have therefore resorted to a numerical study of finite lattices.

Rather than performing a brute force calculation of all the eigenvalues for all complex q (which would not be very illuminating), we have numerically located the zeros of $Z_N(q)$. As is explained in § 3, they must lie on the contours where the largest two eigenvalues cross (apart from a fixed number of isolated zeros). Thus we obtain a cut q plane, within which Λ_1 is the largest eigenvalue, and within which our previous result applies.

Extrapolating to large values of n, this enables us to approximately divide the q plane into three domains $\mathscr{D}_1$, $\mathscr{D}_2$, $\mathscr{D}_3$, within which $W(q)$ is analytic.

We had a problem with the result (Baxter 1986) in that it took three different analytic forms for different ranges of q. These forms are not analytic continuations of one another and it was not clear precisely what the ranges were (nor indeed whether Λ_1 was the largest eigenvalue anyway). Now we can identify these three expressions with $W(q)$ in the three domains $\mathscr{D}_1$, $\mathscr{D}_2$, $\mathscr{D}_3$, respectively. This is done in equations (4.7) and (4.2). Thus the function $W(q)$ is piecewise analytic.

Moreover, now we can exactly locate the boundaries of $\mathscr{D}_1$, $\mathscr{D}_2$, $\mathscr{D}_3$: in § 4 it is shown that they must be the lines where the expressions for $W(q)$ (in the adjacent domains) have equal modulus. The complex zeros of $Z_N(q)$ (for N large) must lie on these lines: we can also determine their limiting distribution. This is done in § 4 and the results indicated in figure 5.

We emphasise that we expect the results to be exact: the only way they could be wrong would be if the domain structure were more complicated. For instance, we cannot rule out the existence of a fourth domain within which $W(q)$ has some yet different form. All we can say is that we have seen no sign of it.

In § 5 we further discuss the finite lattice numerical results and remark that the distributions of the complex zeros do appear to be converging (as the lattice size increases) to those of our infinite-lattice analytic calculations. This is evident in figures 3 and 6. In particular, there are complex zeros near $q = 0$ and $q = 4$, but they are very sparsely distributed. This is a reflection of the fact that W has weak singularities (all its derivatives exist but W is not analytic) at these points. There is a dense line of zeros vertically crossing the real axis at a point F between $q = 2.5$ and 4.0.

The finite lattice results also reveal the presence of isolated real zeros of $Z_N(q)$ at the Beraha numbers to the left of F. As n increases, F moves to the right, so that for

an eight-column lattice (with cylindrical boundary conditions) F is about $q = 3.4$ and one sees the first six Beraha numbers ($r = 2, 3, \ldots, 7$ in (1.1)).

For an infinitely large lattice, the point F in figure 5 is at $q = q_0$, where

$$q_0 = 3.819\,67\ldots$$
$$= 2 + 2\cos(2\pi/14.6834\ldots) \tag{1.4}$$

so that ultimately we expect the first thirteen Beraha numbers ($r = 2, \ldots, 14$) to occur for the triangular lattice.

All the finite lattice results reported in §§ 3-5 are for the $m \times n$ triangular lattice of figure 1, with either free boundary conditions or with cylindrical (right-to-left) boundary conditions, where column n is regarded as followed by column 1. Section 5 ends with a tentative discussion of the possible effects of toroidal boundary conditions.

Finally, for comparison some corresponding results for the honeycomb and square lattices are given in § 6. As one might expect, the zeros are not so smoothly distributed as those for the solvable triangular lattice case.

2. Transfer matrices

The transfer matrix method is well known in statistical mechanics (Baxter 1982) as a technique for simplifying partition functions and it can be applied to the chromatic polynomial (Biggs 1976, Martin 1986, 1987, Mattis 1987). Here we show how to build up the matrix for the triangular lattice dichromatic polynomial (or Potts model) of which the chromatic polynomial is a special case.

Consider the $m \times n$ triangular lattice $\mathscr{L}$ shown in figure 1. It has $N = nm$ sites. It may have free boundary conditions (i.e. be as drawn), or it may have cylindrical boundary conditions (where columns n and 1 are linked by an additional column of m horizontal and $m - 1$ diagonal edges). The possible effect of using toroidal boundary conditions is discussed in § 5.

Consider a general Potts model on $\mathscr{L}$ (Wu 1982). With each site i of $\mathscr{L}$ associate a 'spin' or 'colour' σ_i that can take the values $1, \ldots, q$ (for the moment we take q to

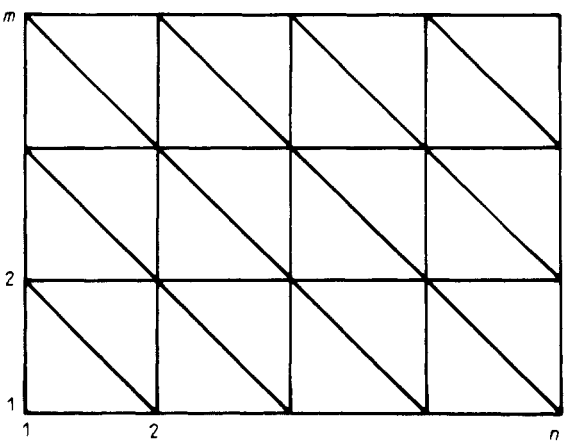

Figure 1. The $m \times n$ triangular lattice with m rows, n columns and $N = mn$ sites.

be a positive integer). The partition function is

$$Z_N(q, v) = \sum_{\sigma} \exp\left(K \sum_{\langle ij \rangle} \delta(\sigma_i, \sigma_j) \right) \tag{2.1a}$$

$$= \sum_{\sigma} \prod_{\langle ij \rangle} (1 + v\delta(\sigma_i, \sigma_j)) \tag{2.1b}$$

where v, K are arbitrary parameters related by

$$v = e^K - 1 \tag{2.2}$$

and where the inner $\langle ij \rangle$ sum and product is over all edges (pairs of nearest-neighbour sites) i, j of $\mathscr{L}$ and the outer σ sum is over all q^N values of all the spins. It is easily seen (Fortuin and Kasteleyn 1972, Baxter *et al* 1976) that (2.1*a*) and (2.1*b*) are equivalent. Further, if G is any graph on $\mathscr{L}$, containing I bonds and C connected components (counting each isolated site as a component), then

$$Z_N(q, v) = \sum_{G} q^C v^I. \tag{2.3}$$

The summation is over all graphs G that can be drawn on $\mathscr{L}$. The expression (2.3) is the dichromatic polynomial of $\mathscr{L}$ (Whitney 1932, Tutte 1967).

As usual, we can express Z_N in terms of a transfer matrix T that adds a row to the lattice $\mathscr{L}$. This matrix can in turn be factored into contributions corresponding to the individual edges. To do this, consider a row of spins $\sigma = \{\sigma_1, \ldots, \sigma_n\}$, with another row $\sigma' = \{\sigma'_1, \ldots, \sigma'_n\}$ above it. Define $q^n \times q^n$ matrices $U_1, \ldots, U_{2n}$, $P_1, \ldots, P_n$, $Q_1, \ldots, Q_n$ by

$$\begin{aligned} (U_{2j-1})_{\sigma\sigma'} &= \prod_{\substack{k=1 \\ \neq j}}^{n} \delta(\sigma_k, \sigma'_k) \\ (U_{2j})_{\sigma\sigma'} &= \delta(\sigma_j, \sigma_{j+1}) \prod_{k=1}^{n} \delta(\sigma_k, \sigma'_k) \end{aligned} \tag{2.4}$$

$$\begin{aligned} P_j &= v\mathbf{1} + U_{2j-1} \\ Q_j &= \mathbf{1} + vU_{2j} \end{aligned} \tag{2.5}$$

where $j = 1, \ldots, n$ and $\sigma_{n+1} \equiv \sigma_1$. It easily verified that

$$\begin{aligned} &U_{2j-1}^2 = qU_{2j-1} \qquad U_{2j}^2 = U_{2j} \qquad U_jU_{j\pm1}U_j = U_j \\ &U_iU_j = U_jU_i \qquad |i-j| \neq 1. \end{aligned} \tag{2.6}$$

In fact $U_1, \ldots, U_{2n}$ are the usual Temperley-Lieb operators (Temperley and Lieb 1971, Baxter 1982, § 12.4), apart from some trivial normalisation factors.

For free boundary conditions, the transfer matrix is then

$$T = P_1Q_1P_2Q_2 \ldots Q_{n-1}P_nH \tag{2.7}$$

where

$$H = Q_1Q_2 \ldots Q_{n-1}. \tag{2.8}$$

(H adds a row of horizontal edges to $\mathscr{L}$; $P_1Q_1 \ldots Q_{n-1}P_n$ adds the vertical and diagonal edges. More specifically, P_j adds a vertical edge in column j; in (2.7) Q_j adds a diagonal edge between columns j and $j+1$, and in (2.8) it adds a horizontal edge.) The partition function is

$$Z_N(q, v) = \xi' H T^{m-1} \xi \tag{2.9}$$

where ξ is the q^n-dimensional column vector with all entries unity, i.e. $\xi(\sigma_1, \ldots, \sigma_n) = 1$.

Cylindrical boundary conditions are more complicated (particularly so because $\mathscr{L}$ is triangular rather than square or honeycomb). They can be handled by considering a lattice of $n+1$ columns (which means replacing n by $n+1$ in (2.4)-(2.8)), and multiplying H by U_{2n+2}. From (2.4) this is equivalent to introducing a factor $\delta(\sigma_{n+1}, \sigma_1)$ in each row, i.e. to identifying column $n+1$ with column 1.

Returning to the n-column case, we make a change of basis as follows. Consider a q^n-dimensional column vector f, of the type that can be formed by successively multiplying ξ by P_j, Q_j and U_j. For $n=3$ its entries $f(\sigma_1, \ldots, \sigma_n)$ have the form

$$f(\sigma_1, \ldots, \sigma_n) = f_1 + f_2\delta(\sigma_1, \sigma_2) + f_3\delta(\sigma_2, \sigma_3) + f_4\delta(\sigma_1, \sigma_3) + f_5\delta(\sigma_1, \sigma_2, \sigma_3) \tag{2.10}$$

where $\delta(a, b, c) = 1$ if $a = b = c$, and 0 otherwise.

For arbitrary n there is a similar expansion as a sum of products of delta functions. Each term in the sum can be represented graphically by a line of n points, with links (on or below the line) joining points i, j if σ_i, σ_j are arguments of the same delta function. The fourteen graphs for $n=4$ are shown in figure 2, for instance the ninth graph denotes the term $\delta(\sigma_1, \sigma_4)\delta(\sigma_2, \sigma_3)$.

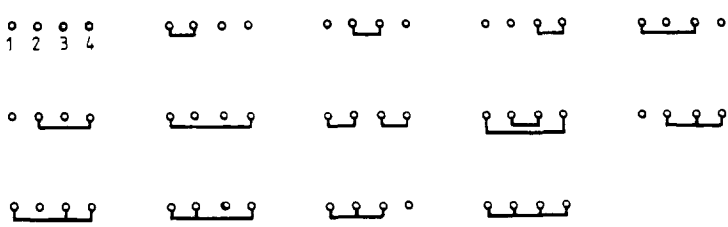

Figure 2. The fourteen graphs consisting of a line of four points (labelled $1, \ldots, 4$ as in the first graph) linked below with no crossed links.

Note that there is no graph in figure 2 corresponding to a term $\delta(\sigma_1, \sigma_3)\delta(\sigma_2, \sigma_4)$. This would be represented by a graph with crossed links: in fact no such crossed link graphs occur (Temperley and Lieb 1971). For general n there are

$$c_n = (2n)!/[n!(n+1)!] \tag{2.11}$$

possible non-crossed graphs, and hence c_n terms in the expansion of $f(\sigma_1, \ldots, \sigma_n)$. These c_n are the Catalan numbers (Sloane 1973, Gardner 1976).

Still considering for definiteness the case $n=3$, consider the effect of premultiplying f by U_1 or U_2. From (2.4) and (2.10)

$$\begin{aligned}(U_1 f)_{\sigma_1,\ldots,\sigma_n} &= qf_1 + f_2 + f_4 + (qf_3 + f_5)\delta(\sigma_2, \sigma_3) \\ (U_2 f)_{\sigma_1,\ldots,\sigma_n} &= (f_1 + f_2)\delta(\sigma_1, \sigma_2) + (f_3 + f_4 + f_5)\delta(\sigma_1, \sigma_2, \sigma_3).\end{aligned} \tag{2.12}$$

Thus $U_1 f$, $U_2 f$ also have elements of the linear form (2.10), and similarly for $U_3, \ldots, U_6$. This gives us a new five-dimensional basis for $U_1, \ldots, U_6$, and in particular we see from (2.12) that

$$U_1 = \begin{pmatrix} q & 1 & 0 & 1 & 0 \\ 0 & 0 & 0 & 0 & 0 \\ 0 & 0 & q & 0 & 1 \\ 0 & 0 & 0 & 0 & 0 \\ 0 & 0 & 0 & 0 & 0 \end{pmatrix} \qquad U_2 = \begin{pmatrix} 0 & 0 & 0 & 0 & 0 \\ 1 & 1 & 0 & 0 & 0 \\ 0 & 0 & 0 & 0 & 0 \\ 0 & 0 & 0 & 0 & 0 \\ 0 & 0 & 1 & 1 & 1 \end{pmatrix}. \tag{2.13}$$

Note also that these matrices are sparse: they have just one non-zero entry in each column, which is one unless it is a diagonal entry of U_{2j-1}, in which case it is q. These properties turn out to apply generally.

In this representation the vector ξ is

$$\xi = \begin{pmatrix} 1 \\ 0 \\ 0 \\ 0 \\ 0 \end{pmatrix} \tag{2.14}$$

while ξ' is no longer the transpose of ξ: premultiplying (2.10) by the original ξ', we find that in the new representation

$$\begin{aligned} \xi' &= (q^3, q^2, q^2, q^2, q) \\ &= (1, 0, 0, 0, 0) U_1 U_3 U_5. \end{aligned} \tag{2.15}$$

Once we have obtained $U_1, \ldots, U_{2n}$, ξ, ξ' in the new representation, we can again use the equations (2.5), (2.7)-(2.9) to evaluate $Z_N(q, v)$. This can be done for any n, but naturally the dimension c_n of the new basis increases with n:

$$c_1, c_2, \ldots = 1, 2, 5, 14, 42, 132, 429, 1430, \ldots. \tag{2.16}$$

Note that q now enters the calculation only as the value of the non-zero diagonal entries of U_1, U_3, $U_5, \ldots$. Thus it can be allowed to take any value, real or complex. Then $Z_N(q, v)$ should be regarded as defined by (2.3).

So far in this section we have considered the general Potts model, where K or v is arbitrary. For the rest of this paper we shall specialise to the case when $K \to -\infty$, i.e. when

$$v = -1. \tag{2.17}$$

The σ summand in (2.1a) is then zero if any two adjacent sites have the same spin (or colour), otherwise it is one. Thus $Z_N(q, -1)$ is the number of ways of colouring $\mathcal{L}$ with q colours, i.e. the chromatic polynomial. We write it simply as $Z_N(q)$.

2.1. Computations

The prime aim of this paper is to analytically discuss the large lattice limit of the polynomial $Z_N(q)$, but in doing so we are guided by the results of various finite lattice calculations. These have been obtained by iteratively evaluating the row vector $f' = \xi' H T^{m-1}$ for increasing values of m. From (2.7) and (2.8), this can be done simply

by successive postmultiplications by $P_1, \ldots, P_n$ and $Q_1, \ldots, Q_{n-1}$ (in correct sequence). Since these matrices (in the new representation) have at most two non-zero entries in each column, the matrix multiplications simplify dramatically. For an arbitrary row vector f', with elements f_j, $j = 1, \ldots, c_n$, we have

$$\begin{aligned}(f'P_r)_j &= -f_j + q^{\lambda_{2r-1,j}} f_{u(2r-1,j)} \\ (f'Q_r)_j &= f_j - f_{u(2r,j)}\end{aligned} \tag{2.18}$$

where $u(r, j)$ is the row location of the non-zero element of U_r in column j, and $\lambda_{rj} = 1$ if $u(r, j) = j$, otherwise $\lambda_{rj} = 0$. Thus one only needs to store the integers $u(r, j)$ and the current set of q polynomials f_j.

A further simplification is that each Q_r is a singular matrix (in fact a projection operator), its column j being zero if $u(2r, j) = j$, as is evident from (2.18). This means that many of the elements of the row vector f' (at any stage in the calculation) will be zero. To maximise the number of such zero elements, it is desirable to multiply by each Q_j as soon as possible (there is some freedom of choice in the sequence, since Q_j commutes with all the other P, Q matrices except P_{j-1} and P_{j+1}). This is achieved by rewriting (2.7) as

$$T = P_1 Q_1 P_2 Q_1 Q_2 P_3 Q_2 \ldots Q_{n-1} P_n Q_{n-1}. \tag{2.19}$$

The coefficients of the polynomials f_j and $Z_N(q)$ are integers. For even modest lattice sizes (e.g. 8×8) they can be very large. It is a help to use $q - 3$ rather than q as a variable, but even then the coefficients can be over sixteen digits long. We handled these efficiently by using FORTRAN and modular arithmetic (Baxter and Enting 1979, p 117). It is important to obtain the coefficients exactly: for example, the polynomials $(x+1)^{64}$ and $(x+1)^{64} - x^{32}$ differ only by one part in 10^{20} in their largest coefficient, yet have completely different distributions of zeros.

3. The infinite strip

Still considering the $m \times n$ triangular lattice of figure 1, we see from (2.9) that

$$Z_N(q) = \sum_r c_{rn}(q) \Lambda_{rn}(q)^m \tag{3.1}$$

where $\Lambda_{rn}(q)$ is the eigenvalue r of the transfer matrix T, and $c_{rn}(q)$ is a coefficient determined by the associated eigenvector. Both are independent of m.

When m is big, the sum in (3.1) will be dominated by the term for which $|\Lambda_{rn}(q)|$ is largest. As q is varied in the complex plane, the two largest eigenvalues may cross (in modulus) at some point q_0. Call the eigenvalues $\Lambda_{1n}(q)$ and $\Lambda_{2n}(q)$. Then in the neighbourhood of q_0

$$Z_N(q) \sim c_{1n}(q) \Lambda_{1n}(q)^m + c_{2n}(q) \Lambda_{2n}(q)^m. \tag{3.2}$$

In general the functions $c_{1n}(q)$, $c_{2n}(q)$, $\Lambda_{1n}(q)$, $\Lambda_{2n}(q)$ will be analytic and non-zero at q_0, so their logarithms can be Taylor expanded in powers of $q - q_0$. It follows that the RHS of (3.2) is a non-zero factor multiplied by

$$\sinh\{i\pi(A + m\phi) + (B + mD)(q - q_0) + O[(q - q_0)^2]\}. \tag{3.3}$$

Here A, B, D are complex numbers independent of m, ϕ is necessarily real and D is in general non-zero.

For m large, the expression (3.3) has zeros close to q_0, at

$$q = q_0 - i\pi[r + A + R(m\phi)]/(mD) \tag{3.4}$$

where $r = 0, \pm 1, \pm 2, \ldots$ and $R(x) = x - [x]$ is x modulo 1. Thus $0 \leqslant R(x) < 1$. In the limit of m large it follows that $Z_N(q)$ has a sequence of zeros close to q_0, evenly spaced on the line where $|\Lambda_{1n}(q)| = |\Lambda_{2n}(q)|$.

Considering the whole plane, it follows for m large that $Z_N(q)$ has a dense distribution of zeros (with spacing proportional to m^{-1}) on the contours $|\Lambda_{1n}(q)| = |\Lambda_{2n}(q)|$, i.e. where the two largest eigenvalues are equimodular. Further, since $\Lambda_{1n}(q)$ is by definition the largest eigenvalue, it cannot be zero (the transfer matrix cannot have all eigenvalues zero), so $Z_N(v)$ can only have zeros when the largest two eigenvalues cross, apart possibly from isolated zeros due to the vanishing of $c_1(v)$.

Now consider figure 3 where the zeros of $Z_N(q)$ are plotted for $n = 5$ and $m = 6, 12$ for a lattice with free boundaries. There are single real zeros at $q = 0, 1, 2.618\ldots$, and a triple zero at $q = 2$. The other zeros are distributed along curves in the complex q plane: as m increases the distribution becomes denser.

Very similar behaviour is observed for other values of m and n and for cylindrical boundary conditions. The behaviour is consistent with the large m analysis given above, and leads one to conclude that the largest transfer matrix eigenvalues (in modulus) cross on curves in the complex plane that are located approximately as in figure 4. (For finite n it is not quite clear whether the curves actually join at B and E, but this does not affect the following discussion.)

The eigenvalues $\Lambda_m(q)$ are algebraic functions of q whose only singularities are branch points. Crossing a branch cut is equivalent to changing from one eigenvalue

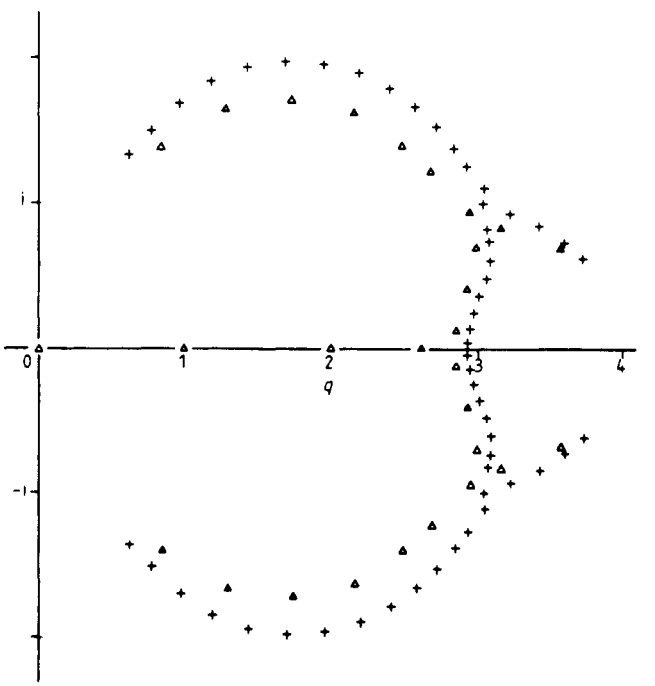

Figure 3. The zeros of the chromatic polynomial $Z_N(q)$ in the complex q plane for two $m \times n$ triangular lattices with free boundaries: △ 6×5 lattice, + 12×5 lattice.

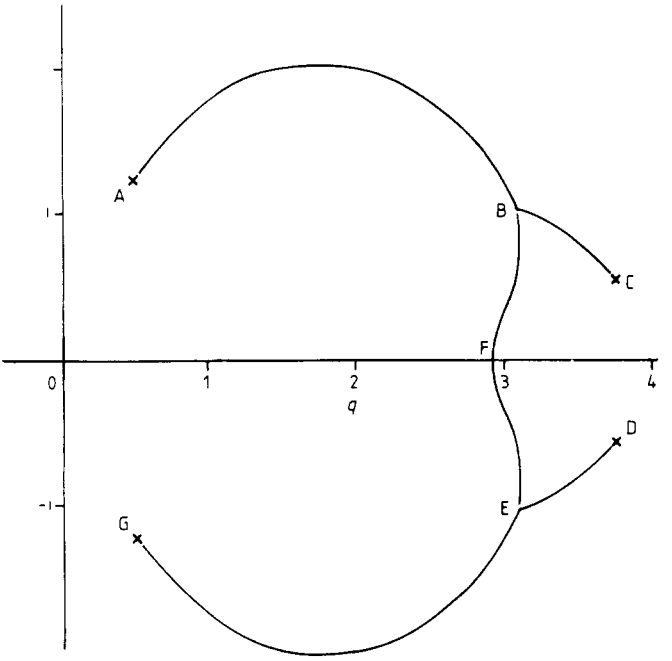

Figure 4. Expected qualitative picture of the cut q plane within which the eigenvalue $\Lambda_{1n}(q)$ is analytic for finite n. (The particular curves shown are based on the $n = 5$ case with free boundaries.) The points A, C, D, G are branch points. There may also be branch points at B and E.

to another. At the branch point ending the cut, the different eigenvalues must be equal. It follows that singularities of the largest eigenvalue $\Lambda_{1n}(q)$ must be associated with the endpoint of a line of zeros of $Z_N(q)$ (for m large). Thus $\Lambda_{1n}(q)$ must be analytic in the q plane cut by the contours formed by the lines of zeros of $Z_N(q)$ in the limit of m large. These branch cut contours must be given by

$$|\Lambda_{1n}^{(+)}(q)| = |\Lambda_{1n}^{(-)}(q)| \tag{3.5}$$

where the supercripts $(+)$ and $(-)$ denote the values of $\Lambda_{1n}(q)$ on either side of the branch cut. Wood (1985, 1987) has used the relation (3.5) to accurately estimate critical points.

We therefore conclude that $\Lambda_{1n}(q)$ is analytic in the cut q plane given qualitatively by figure 4. In the next section we shall show that this is consistent with our previous Bethe ansatz calculations. Further, the results of these calculations can be used to exactly locate ABC, DEG and BE in the limit of m and n large, and to obtain the limiting distribution of zeros on these curves.

4. Bethe ansatz results

In the earlier paper (Baxter 1986) we used the Bethe ansatz to obtain equations for $\Lambda_{1n}(q)$. They involve as intermediate variables a set of 'wavenumbers' $k_1, \ldots, k_n$: there are many solutions, corresponding to the different eigenvalues.

For q real, we found a solution (for n large but finite) where $k_1, \ldots, k_n$ are real and distributed smoothly over some interval $(-Q, Q)$. For q large (positive or negative), it is readily verified that this gives the largest eigenvalue $\Lambda_{1n}(q)$. This solution can be followed to all real values of q by varying q and $k_1, \ldots, k_n$ continuously. Since we expect $\Lambda_{1n}(q)$ to be analytic in the cut plane of figure 4, the Bethe ansatz solution should indeed give $\Lambda_{1n}(q)$ for all real q, *provided* that to the left of BE we use the continuation from the left (i.e. from q negative), while to the right we use the continuation from the right (from q positive large).

Further, the crossover point where one switches from the left-solution to the right-solution is given by (3.4), where (+) and (−) refer to the two solutions. It is the point where the two eigenvalues cross.

Now we take the limit of n large. The Bethe ansatz equations can then be solved explicitly by Fourier transforms. Define x, θ by

$$\begin{aligned} &q = 2 - x - x^{-1} = 2 + 2\cos\theta \\ &|x| < 1 \qquad 0 < \mathrm{Re}(\theta) < \pi \end{aligned} \tag{4.1}$$

and define three functions $g_1(q)$, $g_2(q)$ and $g_3(q)$ by

$$g_1(q) = -\frac{1}{x}\prod_{j=1}^{\infty}\frac{(1-x^{6j-3})(1-x^{6j-2})^2(1-x^{6j-1})}{(1-x^{6j-5})(1-x^{6j-4})(1-x^{6j})(1-x^{6j+1})} \tag{4.2a}$$

$$\ln g_2(q) = \int_{-\infty}^{\infty} \mathrm{d}k \frac{\sinh k\theta}{2k}\left(\frac{\sinh[k(\pi-2\theta)/2]}{[\sinh(\pi k/2)](2\cosh k\theta - 1)} - \frac{\cosh[k(\pi-2\theta)/2]}{[\cosh(\pi k/2)](2\cosh k\theta + 1)}\right) \tag{4.2b}$$

$$\ln g_3(q) = \int_{-\infty}^{\infty} \mathrm{d}k \frac{\sinh k\theta \sinh[k(\pi-\theta)]}{k \sinh \pi k\,[2\cosh k(\pi-\theta) - 1]}. \tag{4.2c}$$

For q real, $q > 4$ or $q < 0$, x is real (its sign is the opposite of q) and so is $g_1(q)$. For $0 < q < 4$, θ is real and so are $g_2(q)$ and $g_3(q)$.

For a large $m \times n$ lattice, with $N = mn$ sites, we want to calculate the partition function per site

$$W(q) = \lim_{N\to\infty} Z_N(q)^{1/N} \tag{4.3}$$

the limit being taken through m, n both large. From (3.1)

$$W(q) = \lim_{n\to\infty} \Lambda_{1n}(q)^{1/n} \tag{4.4}$$

provided $\Lambda_{1n}(q)$ is the largest (in modulus) eigenvalue of the transfer matrix and $c_{1n}(q) \neq 0$.

The formulae (4.2) were obtained in the previous paper (equations (1.7), (1.9) and (5.3) of Baxter (1986)) as expressions for $W(q)$ but it was not clear what their respective ranges of validity were. Now we can be precise. Take q to be real and $\Lambda_{1n}(q)$ to be the abovementioned eigenvalue, with $k_1, \ldots, k_n$ distributed over the interval $(-Q, Q)$. Then the limiting large-n value of $\Lambda_{1n}(a)^{1/n}$ is $g_1(q)$ provided $q > 4$ or $q < 0$. For $0 < q < 4$, $g_2(q)$ is the nth root of the right-continuation of $\Lambda_{1n}(q)$, while $g_3(q)$ is the root of the left-continuation. Thus

$$\begin{aligned} W(q) &= g_1(q) \qquad q > 4 \quad \text{or} \quad q < 0 \\ &= g_2(q) \qquad q_0 < q < 4 \\ &= g_3(q) \qquad 0 < q < q_0. \end{aligned} \tag{4.5a}$$

Here

$$q_0 = 3.819\,67\ldots \tag{4.5b}$$

is defined by

$$g_2(q_0) = g_3(q_0). \tag{4.6}$$

The results (4.5*a*) fail if $c_{1n}(q) = 0$, which happens at the isolated real zeros of $Z_N(q)$. This point is discussed in the next section.

The function $W(q)$ thus defined has a discontinuity in its derivative at $q = q_0$. It also has weak singularities at $q = 0$ and $q = 4$, where it has continuous derivatives of all orders but is not analytic. Such singularities are typical of Bethe ansatz calculations (Lieb and Wu 1972). This is consistent with the fact that, as n increases, the branch points A,F and C,D in figure 4 close in on the real axis at $q = 0$ and $q = 4$, dividing the complex plane into three domains $\mathscr{D}_1$, $\mathscr{D}_2$, $\mathscr{D}_3$, as in figure 5. Within these domains $\Lambda_{1n}(q)$ is analytic, so we expect to be able to analytically continue the results (4.5) throughout the relevant domains, giving

$$W(q) = g_i(q) \qquad \text{in domain } \mathscr{D}_i \qquad i = 1, 2, 3. \tag{4.7}$$

4.1. Location of the lines of zeros ($N \to \infty$)

The boundaries of $\mathscr{D}_1$, $\mathscr{D}_2$, $\mathscr{D}_3$ are the lines occupied by the zeros of $Z_N(q)$ in the large lattice limit. From (3.4) and (4.4), they are given by the requirement that $|W((q)|$ be continuous across them. Thus BAE is given by

$$|g_1(q)| = |g_3(q)|. \tag{4.8}$$

Similarly, BCE is given by $|g_1(q)| = |g_2(q)|$ and BE by $|g_2(q)| = |g_3(q)|$.

We can also obtain the limiting distribution of zeros along these lines by noting that for m large they are the zeros of the RHS of (3.2), $\Lambda_{1n}(q)$ and $\Lambda_{2n}(q)$ being the largest eigenvalues on the two sides of the domain boundary. In the limit of m large we can ignore the contributions from $c_{1n}(q)$ and $c_{2n}(q)$. Along BAE it follows that the zeros are the solutions of

$$g_1(q)^N + g_3(q)^N = 0. \tag{4.9}$$

Similarly, along BCE they are solutions of $g_1(q)^N + g_2(q)^N = 0$, and on BE, of $g_2(q)^N + g_3(q)^N = 0$. Note that these zeros must lie precisely on the boundaries $|g_i(q)| = |g_j(q)|$.

For complex values of q, the functions $g_2(q)/g_1(q)$ and $g_3(q)/g_1(q)$ can be somewhat simplified by evaluating the integrals in (4.2) by summing over poles in the upper half k plane. It turns out that the contributions from the poles at $k = \mathrm{i}r$ (r an integer) exactly cancel the denominator $g_1(q)$.

If we take $\mathrm{Im}(\theta) < 0$, $\mathrm{Im}(q) > 0$, and define

$$p = -\exp(\mathrm{i}\pi^2/3\theta) \qquad y = \exp(-2\mathrm{i}\pi^2/3(\pi - \theta)] \qquad \omega = \exp(2\pi\mathrm{i}/3) \tag{4.10}$$

then we obtain

$$\begin{aligned} g_2(q)/g_1(q) &= \prod_{j=1}^{\infty} \left(\frac{1-\omega p^{2j-1}}{1-\omega p^{2j}}\right)^3 \frac{1-p^{6j}}{1-p^{6j-3}} \\ g_3(q)/g_1(q) &= \prod_{j=1}^{\infty} \left(\frac{1+\omega^2 y^j}{1-\omega^2 y^j}\right)^3 \frac{1-y^{3j}}{1+y^{3j}}. \end{aligned} \tag{4.11}$$

In figure 5 we have plotted the domain boundaries (4.8), etc, together with the solutions of (4.9), etc, for $N = 80$. This gives a coarse-grained picture of the limiting large-N distribution of zeros: one can interpret the line interval between two successive points as containing $\frac{1}{80}$ of all the complex zeros of $Z_N(q)$. This is a convenient way of displaying the distribution: it can be compared directly with finite lattice results.

The point B, where $|g_1(q)| = |g_2(q)| = |g_3(q)|$, is at $q \simeq 4.100 + 0.650\mathrm{i}$, corresponding to $\theta \simeq 0.509 - 0.626\mathrm{i}$. Along the curves BA, BC, BF the arguments of $g_1(q)/g_3(q)$, $g_2(q)/g_1(q)$ and $g_3(q)/g_2(q)$ range monotonically over the intervals $(-v_1, 0)$, $(-v_2, 0)$ and $(v_1 + v_2, \pi)$, respectively, where $v_1 = 2.3624\ldots$ and $v_2 = 0.1223\ldots$. The total range of variation is therefore π, so the equations (4.9), etc, have the correct number of solutions, i.e. $N/2$ above the real axis and $N/2$ below.

Note that $g_3(q)/g_1(q)$ involves θ only via the parameter y. Incrementing $\pi/(\pi - \theta)$ by $3k$, for any integer k, leaves y unchanged. It follows that the curve BAE in figure 5 is just one of an infinite family of curves on which (4.8) is satisfied. The other curves lie inside BAE and rapidly converge on the point $q = 0$.

Similarly, there are curves obtainable from BCE by incrementing π/θ by $6k$, which leaves p and $g_2(q)/g_1(q)$ unchanged. These lie to the left of BCE and converge on $q = 4$. We have ignored those alternative curves as the finite lattice calculations give no evidence of there being zeros on them, and the full set of complex zeros just fits onto BAE, BCE, BFE.

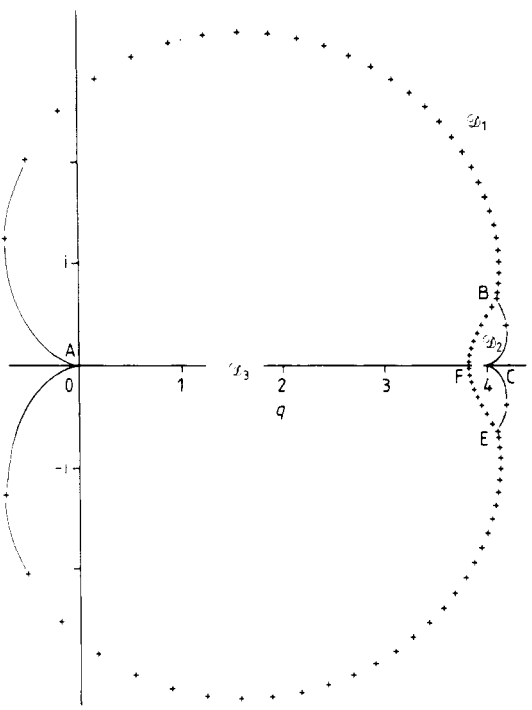

Figure 5. Chromatic zeros in the large lattice limit: the curves and points obtained by solving (4.8), etc, and (4.9), etc (with $N = 80$). The points lie on the curves, and for clarity the curves are only drawn where the points are sparse. When $N \to \infty$ the complex zeros are continuously distributed along the curves, their density being proportional to the density of the points shown. Note that the curves divide the complex q plane into three domains $\mathscr{D}_1$, $\mathscr{D}_2$ and $\mathscr{D}_3$.

5. Finite lattice results

It is interesting to compare the limiting large lattice analytic results of § 4 with those of finite $m \times n$ triangular lattices, where $m \sim n$. In the appendix we give the chromatic polynomials (in powers of $q-3$) of the 6×6 and 8×8 lattices with free and cylindrical boundary conditions. The zeros of three of these polynomials are plotted in figure 6.

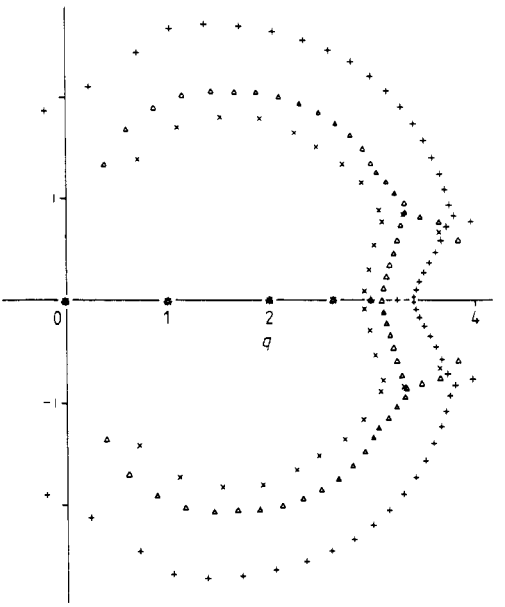

Figure 6. Finite lattice numerical results: chromatic zeros for $m \times n$ triangular lattices with free and cylindrical boundaries: × 6×6, △ 8×8 free, + 8×8 cylindrical. They should be compared with the infinite lattice analytic results of figure 5.

The first point to notice is that the complex zeros plainly lie on smooth curves, unlike, for instance, the zeros of the three-state Potts model (Martin 1985). This seems to be true generally, at least for $m, n \geq 5$, except that with cylindrical boundary conditions we have seen a couple of exceptional points on the right when $n = 5$ or 7. This may be connected with the fact that the three-sublattice structure of the triangular lattice (which ensures that it is three-colourable) is broken if cylindrical boundary conditions are imposed for n not a multiple of 3. It would be interesting to look at a nine-column cylindrical lattice, but this would involve local transfer matrices of dimension $c_{10} = 16\,796$, which would be a comparatively major task. (Typically our computer runs have taken tens of seconds on a shared VAX.)

The zeros shown in figure 6 are not particularly close to the infinite lattice results of figure 5, but they do get closer as the lattice size increases. In particular, note that the cylindrical lattice results are significantly closer than the free ones. This fits with the well known observation in statistical mechanics that periodic boundary conditions greatly reduce finite-size effects. Toroidal boundary conditions (discussed later in this section) would presumably reduce them further. The cylindrical conditions can be thought of as a 'halfway house' to fully periodic toroidal conditions, and indeed the corresponding zeros in figure 6 do lie about midway between those of the free boundaries finite lattice results, and those of the infinite lattice.

Note also that the distribution of zeros in figure 6 is similar to the limiting distribution pictured in figure 5: they are densest along the near-vertical curve near $q = 3$ (the line BE in figure 5), very sparse near $q = 0$ (on BAE) and $q = 4$ (on BCE). This sparsity of zeros is related to the weakness of the singularities of $W(q)$ at $q = 0$ and $q = 4$.

5.1. Beraha numbers

So far we have discussed only the lines of zeros in the complex plane, corresponding to the crossing of transfer matrix eigenvalues. However, in the finite lattice numerical results, isolated real zeros have been observed at or near $q = 0$, 1, 2, 2.618, 3, 3.247. These are the first six of the 'Beraha numbers':

$$B_r = 2 + 2\cos(2\pi/r) \qquad r = 2, 3, 4, \ldots . \tag{5.1}$$

Beraha (Beraha *et al* 1978, 1980) has conjectured that some of the real zeros of chromatic polynomials of planar graphs should, in the limit of the graph becoming large, occur at points in the sequence (5.1). Certainly this is happening in those calculations. The zeros at $q = 0, 1, 2$ are exact for finite n, due simply to the fact that three colours are needed to colour the triangular lattice. (For $m, n \geqslant 3$ these zeros are simple, except that with free boundary conditions the $q = 2$ zero is a triplet.)

As the lattice size increases, zeros appear close to the higher Beraha numbers. The real zeros greater than 2 of some finite lattices are shown in tables 1 and 2. It can be seen that a single zero near

$$B_5 = 2.618\,033\,988\,749\,89\ldots \tag{5.2}$$

appears for quite small lattices and tends rapidly to B_5 as the lattice size increases. (It is not necessary for both m and n to tend to infinity: the zero tends to B_5 as $m \to \infty$ for fixed $n \geqslant 4$.)

For cylindrical boundary conditions with n not a multiple of 3, there is an exact zero at $q = B_6 = 3.0$. However, this is rather trivial as it is just a consequence of the

Table 1. Real zeros greater than 2 of chromatic polynomials of $m \times n$ triangular lattices with cylindrical boundary conditions, together with the intercept F of the line BE of complex zeros with the real axis. Note the rapid convergence of the zeros to the Beraha numbers B_5, B_6, B_7.

m	n	First zero	Second zero	Third zero	F
4	4	2.617 986 010 522	3.0‡§		
5	4	2.618 032 967 355	3.0‡‖		
5	5	2.618 033 990 394	3.0‡		
6	5	2.618 033 988 754	3.0‡		3.19
6	6	2.618 033 988 750	3.001 033 706		3.13
7	6	2.618 033 988 750	3.000 125 270		3.15
7	7	2.618 033 988 750	3.0‡	3.247 001 349	3.40
8	7	2.618 033 988 750	3.0‡	3.246 981 116	3.42†
8	8	2.618 033 988 750	3.0‡	3.246 979 602	3.40†
9	8	2.618 033 988 750	3.0‡	3.246 979 604	3.42†

† Extrapolation.
‡ Exact.
§ Triple zero.
‖ Quadruple zero.

Table 2. The same data as for table 1, but with free boundary conditions.

m	n	First zero	Second zero	F
4	4	2.604 661 945 742		
5	4	2.616 620 513 049		
5	5	2.618 161 303 055		2.80
6	5	2.618 032 144 827		2.85†
6	6	2.618 033 979 731		2.92†
7	6	2.618 033 988 710		2.95†
7	7	2.618 033 988 750		2.98
8	7	2.618 033 988 750	3.011 865 723	3.03
8	8	2.618 033 988 750	3.000 359 694	3.10
9	8	2.618 033 988 750	3.000 019 560	3.13

† Extrapolation.

boundary conditions being mismatched for a three-colouring of the lattice. What is more interesting is that there is a single zero close to B_6 when $n=6$ and $m \geqslant 5$, and for free boundary conditions when $n \geqslant 7$ and $m \geqslant 8$. Again, they are converging rapidly (to B_6) as m increases (for fixed n). For the lattice with $n=6$ columns and cylindrical boundary conditions, the numerical evidence (for $m=5,\ldots,12$) strongly suggests that $q-3 \propto 8^{-m}$ for m large.

For cylindrical boundary conditions, with $n \geqslant 7$ and $m \geqslant 5$, we also see a single zero approaching

$$B_7 = 3.246\,979\,6037\ldots. \tag{5.3}$$

Provided m, n are sufficiently large ($\geqslant 5$ for free boundary conditions, $\geqslant 6$ for cylindrical), the complex zeros form a pattern recognisably that of figures 3 and 6. There is a line BE of zeros vertically cutting the real axis at a point F between $q=2$ and 4. The value of q at F is also given in tables 1 and 2. There may or may not be a real zero actually at F: if there is not, we have obtained its value (denoted by †) by extrapolation from the nearby complex zeros. Notice that F generally increases with lattice size and there are never any real zeros to the right of F.

Our numerical calculations are of course limited by computer time, so we have not calculated the chromatic zeros of lattices with more than eight columns. We have therefore not observed an isolated zero converging to $B_8 = 3.4142\ldots$ (or to any higher Beraha number) since F is not significantly larger than this even for the seven- and eight-column lattices with cylindrical boundary conditions. It seems likely that one would see such a zero for the nine-column lattice.

As the lattice size increases (in both directions), it appears that the line BFE of zeros moves to the right, successively 'uncovering' Beraha number zeros as it does so. We can understand this in terms of (3.2), taking $\Lambda_{1n}(q)$ therein to be the 'left' eigenvalue obtained by continuation from negative values of q and $\Lambda_{2n}(q)$ to be the 'right' eigenvalue obtained by continuation from $q>4$. If $c_{1n}(q)$ has the Beraha numbers as zeros, while $c_{2n}(q)$ does not, then the Beraha numbers will be (for m large) zeros of $Z_N(q)$ only if they lie in the domain $|\Lambda_{1n}(q)| > |\Lambda_{2n}(q)|$, i.e. to the left of BFE. It may well be that, for n large, $c_{1n}(q)$ has all the Beraha numbers as zeros.

From (4.5*b*), the large lattice limit of the intersection F of BE with the real axis is at $q=q_0$, where q_0 is given by (1.4). It lies between B_{14} and B_{15}, so we expect only the Beraha numbers $B_2,\ldots,B_{14}$ to be the real zeros of the triangular lattice chromatic

polynomial. If $c_{1n}(q) = 0$, the forms (4.3) then it is discontinuous at the Beraha numbers $B_2, \ldots, B_{14}$, having there the value zero; otherwise it is given by (4.5*a*).

5.2. Tutte's golden ratio theorem

The Beraha number B_5 is equal to $1+\tau$, where

$$\tau = (1+\sqrt{5})/2 = 1.618\ldots \tag{5.4}$$

is the 'golden ratio'. Quispel has alerted the author to a theorem of Tutte (1970), which states that if $\mathscr{L}'$ is a triangulation of the sphere and $Z'_N(q)$ is the chromatic polynomial of $\mathscr{L}'$ (where N is the number of sites of $\mathscr{L}'$), then

$$|Z'_N(1+\tau)| \leqslant \tau^{5-N}. \tag{5.5}$$

In fact our lattice $\mathscr{L}$ is not a triangulation of the sphere, since the exterior faces are not triangles. However, we can modify the $m \times n$ lattice $\mathscr{L}$ with cylindrical boundary conditions to become such a triangulation. We do this by adding at the top a 'cap' consisting of a single new site connected to all the sites in the top row, and similarly at the bottom. The new lattice $\mathscr{L}'$ has $2+mn$ sites.

We calculated $Z_N(1+\tau)$ exactly for both $\mathscr{L}$ and $\mathscr{L}'$, expressing it in the form $(a+b\tau)\tau^{-k}$, where a, b and k are integers; a and b have the same sign and $0 \leqslant |b| < |a|$. (This can be done by repeated use of $\tau^2 = \tau + 1$.) We did this for $1 \leqslant m \leqslant 8$ and $3 \leqslant n \leqslant 7$, and for all these values we observed an intriguing property:

$$Z_{mn}(1+\tau) = \tau^{2n-2} Z'_{2+mn}(1+\tau) \tag{5.6}$$

n being the number of columns of $\mathscr{L}$ and $\mathscr{L}'$.

We have no proof of this relation, but assuming it to hold generally, it follows from (5.5) that

$$|Z_{mn}(1+\tau)| \leqslant \tau^{1+2n-nm} \tag{5.7}$$

for the $m \times n$ triangular lattice with cylindrical boundary conditions.

This is really quite a remarkable result. For example, for a 7×7 lattice, $Z_N(q)$ (expressed as a polynomial in $q-3$) has integer coefficients as large as 10^{12}. Yet the RHS of (5.7) is then of order 10^{-7}!

We of course find that (5.7) is satisfied. In fact for the 6×6, 7×7 and 8×8 lattices the ratio of the LHS to the RHS of (5.7) is 0.246×10^{-2}, 0.791×10^{-5} and -0.176×10^{-5}, respectively. Thus $|Z_N(1+\tau)|$ is even smaller than Tutte's theorem requires.

Another interesting property that was observed (again prompted by Quispel) concerned the m dependence for given n. Still considering cylindrical boundary conditions, for $n = 3$ and general q,

$$Z_{m3}(q) = q(q-1)(q-2)(q^3 - 9q^2 + 29q - 32)^{m-1}. \tag{5.8}$$

The simple power law dependence on m is due to the fact that the transfer matrix simplifies to being one-by-one, so there is only one term in the summation in (3.1). For $n > 3$ this is not the case for general q, but we observed from our exact integer arithmetic calculations that

$$\begin{aligned} Z_{m3}(1+\tau) &= 2^{m-1}\tau^{7-5m} \\ Z_{m4}(1+\tau) &= 2^m \tau^{11-8m} \\ Z_{m5}(1+\tau) &= (2+\tau)(-3)^{m-1}\tau^{12-10m}. \end{aligned} \tag{5.9}$$

Thus for $q = 1 + \tau$ there is still only one non-zero term in the sum (3.1), even for $n = 4$ and $n = 5$.

For free boundaries $Z_N(1+\tau)$ is still small, though in general not as small as for the cylindrical case. For the 5×5, 6×6, 7×7 and 8×8 lattices (with $N = 25, 36, 49$ and 64), the values of $\tau^{N-5} Z_N(1+\tau)$ are 5.658, 2.952, 2.058 and 0.852, respectively.

5.3. Toroidal boundary conditions

It would be interesting to repeat these calculations with toroidal boundary conditions. We have not yet done so because the calculation is considerably more complicated: one has to calculate the trace of T^m, instead of a single matrix element. Even more seriously, one can no longer restrict attention to vectors f with elements of the form (2.10) (or its generalisation to higher n). One has to consider all possible forms of $f(\sigma_1, \ldots, \sigma_n)$.

For these reasons, considerably more coding would be required and calculation time would be greatly increased. The author's guess is that the complex zeros would still form patterns similar to those of figure 6, but much closer to the infinite lattice limiting distribution of figure 5.

The chromatic polynomial is now given by $Z_N(q) = \mathrm{Tr}\ T^m$, so (3.1) is replaced by

$$Z_N(q) = \sum_r \Lambda_{rn}(q)^m. \tag{5.10}$$

At first sight one would conclude that the isolated Beraha number zeros no longer occur, since we associated them with the zeros of the coefficient $c_{1n}(q)$ in (3.1). However, this argument would apply equally well to the cylindrical top-to-bottom lattice, which by symmetry has the same $Z_N(q)$ as the cylindrical right-to-left lattice discussed above, and which certainly does have isolated Beraha number zeros.

The explanation may be connected with the fact that the eigenvalues are degenerate, with degeneracies proportional to

$$d_r = \sin(r\theta/2)/\sin(\theta/p) \qquad r = 1, 2, 3, \ldots \tag{5.11}$$

where θ is given by (4.1), and $p = 1$ if r is even or $p = 2$ if r is odd. (Kelland (1976) has observed such degeneracies in a corner transfer matrix calculation on the Potts model.) These d_r are polynomials in q and are integers if q is an integer. For general values of q (in particular at the Beraha numbers $\theta = 2\pi/r$) they can vanish, so this may provide a mechanism for (or at least be connected with) the occurrence of zeros of $Z_N(q)$ at the Beraha numbers.

6. Other planar lattices

The colouring problem is 'solvable' on the triangular lattice, in the sense that $Z_N(q)^{1/N}$ has been exactly calculated in the large lattice limit, being given by (4.2) and (4.5). The same has not been done for the honeycomb and square lattices. It is interesting to look at the distribution of the zeros of their chromatic polynomials, to see if they appear more complicated (and hence less likely to be amenable to exact solution) then those for the triangular lattice.

The $m \times n$ square lattice can be obtained from the $m \times n$ triangular lattice of figure 1 by deleting all diagonal edges and the honeycomb (or 'brick') lattice by further deleting alternate vertical bonds. The results for the 8×8 lattices thus obtained, with

both free and cylindrical boundary conditions, are plotted in figures 7 and 8. For free boundaries the distributions are much less regular than for the triangular lattice. For cylindrical boundaries the zeros appear to be settling down onto fairly smooth curves (particularly for the square lattice). This is not surprising: as has been remarked by Wood (1985, 1987), and in § 3 of this paper, in the limit of m large the zeros should be distributed along the contours $|\Lambda_{1n}| = |\Lambda_{2n}|$ (apart from a fixed number of isolated zeros). They are still not as smoothly distributed as those of the triangular lattice.

The distributions of zeros are further to the left than those for the triangular lattice, so the only Beraha number zeros we have observed in our calculations on the square and honeycomb lattices (of up to eight columns) are the trivial zeros at $q = 0$ and $q = 1$ and a zero converging on $q = 2$. We have not observed any zero close to B_5.

For the honeycomb lattice with cylindrical boundary conditions there is a pair of complex conjugate zeros converging on the real axis at a point $q \simeq 1.7372$. In figure 8 they appear as a single point on the real axis.

Our results for the square 2×15 lattice with cylindrical boundary conditions agree with those plotted by Biggs *et al* (1972). For the square and honeycomb lattices we expanded the chromatic polynomials in powers of $q-2$, rather than $q-3$ as the triangular case.

At the end of § 2 we remarked on the need to calculate exactly the integer coefficients of the chromatic polynomials. Correspondingly, it is necessary to use a high degree of precision in calculating their zeros. All the plots shown in figures 3, 6, 7 and 8 were obtained using both double (16 significant figures) and quadruple (34 figures) precision.

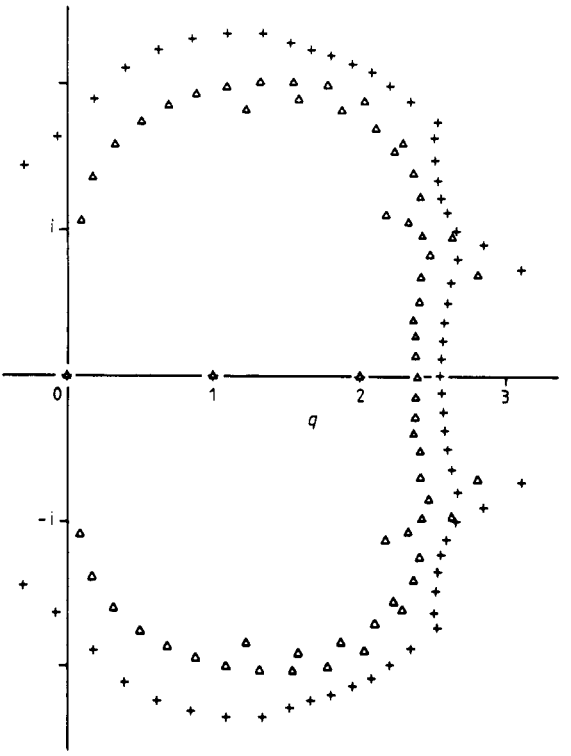

Figure 7. Chromatic zeros for 8×8 square lattices (with 64 sites): △ free boundary conditions, + cylindrical boundary conditions.

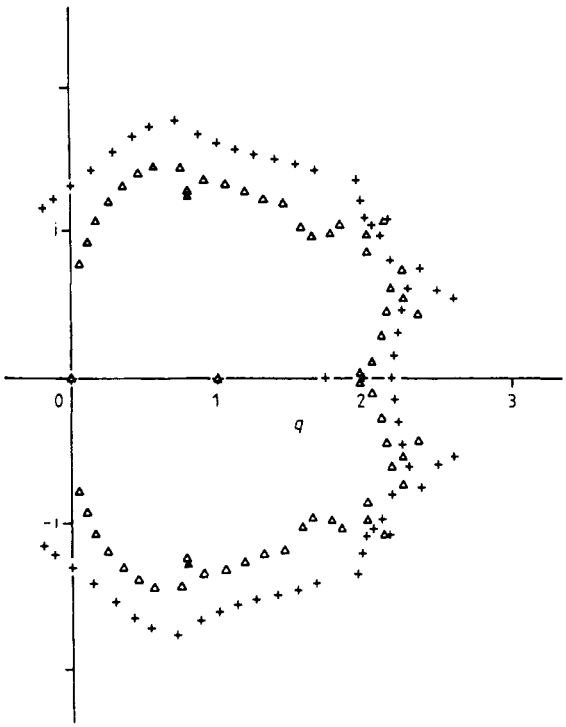

Figure 8. Chromatic zeros for 8×8 honeycomb lattices (with 64 sites): $\triangle$ free boundary conditions, + cylindrical boundary conditions.

For the 8×8 honeycomb free case (which has coefficients as large as 10^{16}) the double precision results were significantly in error. (For the other plots double precision was in fact adequate.)

7. Summary

For the triangular lattice colouring problem, we have exactly obtained the partition function per site $W(q) = Z_N(q)^{1/N}$, in the limit of N large, for complex values of q. It is a piecewise analytic function, being analytic inside the three domains $\mathcal{D}_1$, $\mathcal{D}_2$, $\mathcal{D}_3$ indicated in figure 5 (except for removable discontinuities at the Beraha numbers inside $\mathcal{D}_3$). It is given by (4.2) and (4.7).

The complex zeros of the chromatic polynomial $Z_N(q)$ are smoothly distributed along the boundaries between these domains, being given (for N large) by (4.9) and its corresponding equations. There are also real zeros at the Beraha numbers (1.1) lying inside $\mathcal{D}_3$, i.e. those with $r = 2, 3, \ldots, 14$. (Provided the lattice has more than two rows and columns the real zeros are simple, except that with free boundary conditions the $q = 2$ zero is a triplet, and the $m \times 4$ lattice with cylindrical boundary has a zero of degree $m - 1$ at $q = 3$.)

Acknowledgment

The author thanks Dr G R W Quispel for alerting him to Tutte's theorem (5.5).

Appendix

Chromatic polynomials, expressed in powers of $\lambda = q-3$, for the 6×6 and 8×8 triangular lattices with free and cylindrical boundary conditions.

Free boundary: $Z_{6\times 6}(\lambda+3) = \lambda^{36} + 23\lambda^{35} + 265\lambda^{34} + 2025\lambda^{33} + 11490\lambda^{32} + 51460\lambda^{31} + 189020\lambda^{30} + 584653\lambda^{29} + 1552753\lambda^{28} + 3595323\lambda^{27} + 7349245\lambda^{26} + 13405898\lambda^{25} + 22032973\lambda^{24} + 32915660\lambda^{23} + 45063686\lambda^{22} + 56962494\lambda^{21} + 66922695\lambda^{20} + 73480554\lambda^{19} + 75722993\lambda^{18} + 73428253\lambda^{17} + 67071484\lambda^{16} + 57670576\lambda^{15} + 46565019\lambda^{14} + 35185510\lambda^{13} + 24739365\lambda^{12} + 16088331\lambda^{11} + 9607796\lambda^{10} + 5207475\lambda^{9} + 2542931\lambda^{8} + 1101492\lambda^{7} + 412967\lambda^{6} + 134011\lambda^{5} + 35294\lambda^{4} + 7333\lambda^{3} + 1201\lambda^{2} + 113\lambda + 6$.

Free boundary: $Z_{8\times 8}(\lambda+3) = \lambda^{64} + 31\lambda^{63} + 497\lambda^{62} + 5425\lambda^{61} + 45038\lambda^{60} + 301876\lambda^{59} + 1695776\lambda^{58} + 8190257\lambda^{57} + 34649815\lambda^{56} + 130240997\lambda^{55} + 439866761\lambda^{54} + 1347118442\lambda^{53} + 3769975297\lambda^{52} + 9704625168\lambda^{51} + 23111424876\lambda^{50} + 51180977461\lambda^{49} + 105885539163\lambda^{48} + 205520234527\lambda^{47} + 375721719836\lambda^{46} + 649320970171\lambda^{45} + 1064422431079\lambda^{44} + 1660407868475\lambda^{43} + 2471974783090\lambda^{42} + 3522029306153\lambda^{41} + 4814368552526\lambda^{40} + 6328047479151\lambda^{39} + 8013834834161\lambda^{38} + 9795246420053\lambda^{37} + 11572530664354\lambda^{36} + 13230615860137\lambda^{35} + 14653879379616\lambda^{34} + 15726338355123\lambda^{33} + 16376898862342\lambda^{32} + 16516826779294\lambda^{31} + 16191161866788\lambda^{30} + 15327459610507\lambda^{29} + 14130684075243\lambda^{28} + 12530820986828\lambda^{27} + 10800229167457\lambda^{26} + 8991992513046\lambda^{25} + 7123018952267\lambda^{24} + 5628680867958\lambda^{23} + 4003285091750\lambda^{22} + 2986185046357\lambda^{21} + 1964376454405\lambda^{20} + 1226915309592\lambda^{19} + 897992497288\lambda^{18} + 343428884399\lambda^{17} + 342795804866\lambda^{16} + 98951234162\lambda^{15} + 49639945093\lambda^{14} + 69898753299\lambda^{13} - 28958806014\lambda^{12} + 33191581535\lambda^{11} - 12222640723\lambda^{10} + 5069853434\lambda^{9} - 3613798748\lambda^{8} - 3558763447 + 3063992186^{6} - 1097788545\lambda^{5} + 272346544\lambda^{4} - 42129393\lambda^{3} + 4022442\lambda^{2} - 16825\lambda + 6$.

Cylindrical boundary: $Z_{6\times 6}(\lambda+3) = \lambda^{36} + 12\lambda^{35} + 90\lambda^{34} + 460\lambda^{33} + 1875\lambda^{32} + 6102\lambda^{31} + 17024\lambda^{30} + 40275\lambda^{29} + 84807\lambda^{28} + 159818\lambda^{27} + 267777\lambda^{26} + 459009\lambda^{25} + 581380\lambda^{24} + 1195436\lambda^{23} + 751358\lambda^{22} + 3096960\lambda^{21} + 321138\lambda^{20} + 4852436\lambda^{19} + 6358229\lambda^{18} - 13524615\lambda^{17} + 53455321\lambda^{16} - 89432823\lambda^{15} + 137671889\lambda^{14} - 126541161\lambda^{13} + 66871236\lambda^{12} + 50533690\lambda^{11} - 136267488\lambda^{10} + 156042739\lambda^{9} - 103989987\lambda^{8} + 41963001\lambda^{7} - 4864626\lambda^{6} - 4083892\lambda^{5} + 2672347\lambda^{4} - 725248\lambda^{3} + 103911\lambda^{2} - 5911\lambda + 6$.

Cylindrical boundary: $Z_{8\times 8}(\lambda+3) = \lambda^{64} + 16\lambda^{63} + 168\lambda^{62} + 1232\lambda^{61} + 7364\lambda^{60} + 36000\lambda^{59} + 153800\lambda^{58} + 567336\lambda^{57} + 1900570\lambda^{56} + 5626328\lambda^{55} + 15612016\lambda^{54} + 38406416\lambda^{53} + 92202268\lambda^{52} + 191369184\lambda^{51} + 417275308\lambda^{50} + 721891686\lambda^{49} + 1533882600\lambda^{48} + 2106881904\lambda^{47} + 4688361388\lambda^{46} + 5506608096\lambda^{45} + 8499164056\lambda^{44} + 2966123418\lambda^{43} - 59181603950\lambda^{42} + 3475862399\lambda^{41} - 10952177123\lambda^{40} + 36798078583\lambda^{39} - 107074645407\lambda^{38} + 296442446597\lambda^{37} - 752582134566\lambda^{36} + 1770271004466\lambda^{35} - 3785584485227\lambda^{34} + 7213638903253\lambda^{33} - 11610525036789\lambda^{32} + 13493009184745\lambda^{31} - 16236481510336\lambda^{30} - 50804746134722\lambda^{29} + 195831441938876\lambda^{28} - 516146213228270\lambda^{27} + 1114287617092575\lambda^{26} - 2070794939983707\lambda^{25} + 3366397758554811\lambda^{24} - 4791761818604503\lambda^{23} + 5907180302980970\lambda^{22} - 6130696132781670\lambda^{21} + 4984998421654371\lambda^{20} - 2415236246684352\lambda^{19} - 1025348474108844\lambda^{18} + 4313957075844697\lambda^{17} - 6418667245717936\lambda^{16} + 6819018316742569\lambda^{15} - 5734756721977255\lambda^{14} + 3911492110580697\lambda^{13} - 2147366125505722\lambda^{12} + 910796704781837\lambda^{11} - 262055038461118\lambda^{10} + 199336466702522\lambda^{9} + 28977032126598\lambda^{8} - 2034367927841030\lambda^{7} + 799957945904272\lambda^{6} - 216732910691760\lambda^{5} + 41460612053648\lambda - 5396426432544\lambda^{3} + 430750185728\lambda^{2} - 15935761920\lambda$.

References

Asano T 1970 *J. Phys. Soc. Japan* **29** 350-9

Baxter R J 1982 *Exactly Solved Models in Statistical Mechanics* (New York: Academic)

—— 1986 *J. Phys. A: Math. Gen.* **19** 2821-39
Baxter R J and Enting I G 1979 *J. Stat. Phys.* **21** 103-23
Baxter R J, Kelland S B and Wu F Y 1976 *J. Phys. A: Math. Gen.* **9** 397-406
Beraha S, Kahane J and Weiss N J 1978 *Studies in Foundations and Combinatorics* ed C G Rota (New York: Academic) pp 213-32
—— 1979 *J. Combin. Theor.* B **27** 1-12
—— 1980 *J. Combin. Theor.* B **28** 52-65
Biggs N L 1976 *J. Combin. Theor.* B **20** 5-19
Biggs N L, Damerell R M and Sands D A 1972 *J. Combin. Theor.* B **12** 123-31
Fortuin C M and Kasteleyn P W 1972 *Physica* **57** 536-64
Gardner M 1976 *Sci. Am.* **234** no 6 120-5
Glasser M L, Privman V and Schulman L S 1987a *Phys. Rev.* B **35** 1841-5
—— 1987b *J. Stat. Phys.* to be published
Izergin A G and Korepin V E 1981 *Commun. Math. Phys.* **79** 303-16
Kelland S B 1976 *PhD Thesis* Australian National University
Lee T D and Yang C N 1952 *Phys. Rev.* **87** 404-9, 410-9
Lieb E H and Wu F Y 1972 *Phase Transitions and Critical Phenomena* vol 1, ed C Domb and M S Green (New York: Academic) pp 321-490
Martin P P 1985 *Integrable Systems in Statistical Mechanics* ed G M d'Ariano, A Montorsi and M G Rasetti (Singapore: World Scientific) pp 129-42
—— 1986 *J. Phys. A: Math. Gen.* **19** L1117-23
—— 1987 *J. Phys. A: Math. Gen.* **20** L399-403
Mattis D C 1987 *Preprint, The q colour problem on a lattice*
Monroe J L 1982 *J. Phys. A: Math. Gen.* **15** 2499-508
—— 1983 *J. Stat. Phys.* **33** 77-89
Nienhuis B 1982 *Phys. Rev. Lett.* **49** 1062-5
—— 1984 *J. Stat. Phys.* **34** 731-61
Ruelle D 1971 *Phys. Rev. Lett.* **26** 303-4
—— 1973 *Commun. Math. Phys.* **31** 265-77
Sloane N J A 1973 *A Handbook of Integer Sequences* (New York: Academic)
Suzuki M and Fisher M E 1971 *J. Math. Phys.* **12** 235-46
Temperley H N V and Lieb E H 1971 *Proc. R. Soc.* A **322** 251-80
Thompson C J 1972 *Mathematical Statistical Mechanics* (Princeton: Princeton University Press) ch 4
Tutte W T 1967 *J. Combin. Theor.* **2** 301-20
—— 1970 *J. Combin. Theor.* **9** 289-96
—— 1973 *Can. J. Math.* **25** 426-47
—— 1982 *Can. J. Math.* **34** 741-58, 952-60
Whitney H 1932 *Ann. Math., NY* **33** 688-718
Wood D W 1985 *J. Phys. A: Math. Gen.* **18** L917-21
—— 1987 *J. Phys. A: Math. Gen.* **20** 3471-93
Wu F Y 1982 *Rev. Mod. Phys.* **54** 235-68